

DYNAMICAL EXPANSION OF IONIZATION AND DISSOCIATION FRONT AROUND A MASSIVE STAR. I. A MODE OF TRIGGERED STAR FORMATION

TAKASHI HOSOKAWA¹ AND SHU-ICHIRO INUTSUKA²
Draft version November 23, 2018

ABSTRACT

We analyze the dynamical expansion of the H II region and outer photodissociation region (PDR) around a massive star by solving the UV and FUV radiation transfer and the thermal and chemical processes in a time-dependent hydrodynamics code. We focus on the physical structure of the shell swept up by the shock front (SF) preceding the ionization front (IF). After the IF reaches the initial Strömgen radius, the SF emerges in front of the IF and the geometrically thin shell bounded with the IF and the SF is formed. The gas density inside the shell is about 10^{1-2} times as high as the ambient gas density. Initially the dissociation fronts expands faster than IF and the PDR is formed outside the H II region. Thereafter the IF and SF gradually overtakes the proceeding dissociation fronts (DFs), and eventually DFs are taken in the shell. The chemical composition within the shell is initially atomic, but hydrogen and carbon monoxide molecules are gradually formed. This is partly because the IF and SF overtake DFs and SF enters the molecular region, and partly because the reformation timescales of the molecules become shorter than the dynamical timescale. The gas shell becomes dominated by the molecular gas by the time of gravitational fragmentation, which agrees with some recent observations. A simple estimation of star formation rate in the shell can provide a significant star formation rate in our galaxy.

Subject headings: Circumstellar matter – H II regions – ISM: molecules – STARS : formation

1. INTRODUCTION

As the H II region expands around a massive star, the shock front (SF) emerges preceding the ionization front (IF). This SF sweeps up the ambient gas and the gas shell is formed at the edge of the H II region. Many authors have studied the scenario that the shell becomes unstable and next star formation is triggered around H II region (collect and collapse model, see, e.g., Elmegreen & Lada 1977, Whitworth et al. 1994, Elmegreen 1998, and references therein). Recently, Deharveng et al. (2003, hereafter DV03) observed the fragmented molecular shell around the classical H II region, Sh104 and show the young stars (cluster) is formed in the core of one fragment. They argue that this is the evidence of collect and collapse model. Now we can refine the theory for the evolution of the shell and compare it with the detailed observation. Especially, we can focus on the amount of the fragmented *molecular* gas they observed. The SF initially emerges in front of the IF, where sufficient FUV photons to dissociate molecules are available. Therefore, it is not clear whether the SF can gather the molecular gas in the shell as observation indicates or not.

Roger & Dewdney (1992) and Diaz-Miller, Franco & Shore (1998) studied the time-dependent expansion of H II and PDR solving the radiative transfer of UV and FUV photons. Although these works do not include hydrodynamics, they have shown that the IF gradually overtakes the dissociation front (DF) and this means that IF and preceding SF gradually enter the molecular region. The numerical study of the hydrodynamical expansion of the IF has been studied since 1960's (e.g. Mathews 1965, Lasker 1966, Tenorio-Tagle 1976, Tenorio-Tagle 1979, Franco et al. 1990 etc.). These works successfully show the various

dynamical aspects of the expansion in both homogeneous and inhomogeneous ambient medium. However, these do not include the outer photodissociation region (PDR) and thermal processes dominant in PDR.

We perform the time-dependent calculation including the IF, DF, and the shell, which has been very limited. We solve the UV and FUV radiation transfer and hydrodynamics numerically to investigate the structure and evolution of the shell and PDR as well as H II region. Since the compression rate behind the SF depends on the thermal processes, we include the thermal processes which dominate either in H II region or PDR. In this letter, we consider the simple situation that there is one massive star within the homogeneous ambient medium, which can be compared with Sh104 observed by DV03. The detailed quantitative aspects of the evolution will be given in subsequent paper (Hosokawa & Inutsuka 2004, hereafter, Paper II).

2. NUMERICAL METHODS

We use a one-dimensional spherically-symmetrical numerical method. The numerical scheme for the hydrodynamics is based on the 2nd-order Lagrangian Godunov method (see, e.g., van Leer 1979). We use the on-the-spot approximation for UV and FUV radiation transfer. We assume that all hydrogen molecules are in the ground vibrational level of $X^1\Sigma_g$ and ortho/para ratio is 3:1 (Diaz-Miller, Franco & Shore 1998). For the Lyman-Werner bands to photodissociate hydrogen molecule, we solve the frequency dependent transfer using the representative set of lines. The UV and FUV photon luminosity of the central star is adopted from Diaz-Miller, Franco & Shore (1998) for the case of $Z = 1Z_\odot$. The main thermal pro-

¹ Yukawa Institute for Theoretical Physics, Kyoto University, Kyoto, Japan, 606-8502 ; hosokawa@yukawa.kyoto-u.ac.jp

² Department of Physics, Kyoto University, Kyoto, Japan, 606-8502 ; inutsuka@tap.scphys.kyoto-u.ac.jp

cesses included in the energy equation is UV/FUV heating (e.g., H photoionization, photoelectric heating) and radiative cooling (e.g., H recombination, Ly- α , OI (63.0 μ m, 63.1 μ m), OII (37.29 μ m), CII (23.26 μ m, 157.7 μ m), H₂, and CO, see Hollenbach & McKee 1979, 1989, Koyama & Inutsuka 2000). Non-equilibrium reaction equations are implicitly solved for the species of e, H, H⁺, H₂, C⁺, and CO. The ionization rate of O is assumed to be the same as that of H. We adopt the simple approximation for the dissociation process of CO molecule given by Nelson & Langer (1997). The hydrodynamic equations and the radiative transfer equation, energy equation, and reaction equations are combined following Tenorio-Tagle (1976). The dust extinction is included only outside the IF and the dust temperature is calculated following Hollenbach, Takahashi & Tielens (1991). We have checked our numerical code with the well-studied problems (e.g., Franco et al. 1990).

3. RESULTS OF THE NUMERICAL CALCULATION

In this letter, we consider one typical case where there is one massive star of $T_{\text{eff}} = 40000$ K ($M = 41 M_{\odot}$) in the ambient medium. This corresponds to the O6V star, which is the central star of Sh104. The initial ambient number density of the hydrogen nucleon is unknown, and we adopt a typical value of the giant molecular cloud, $n_{\text{H},0} = 10^3 \text{ cm}^{-3}$ ($n_{\text{H}_2,0} = 500 \text{ cm}^{-3}$). As in the standard picture (e.g. Spitzer 1978), the IF expands rapidly as the weak R-type front in the recombination timescale, $t_{\text{rec}} \sim 100 \text{ yr}$ for $n_{\text{H},0} = 10^3 \text{ cm}^{-3}$ (formation phase). As the IF reaches Strömngren radius, $R_{\text{st}} = 0.56 \text{ pc}$, the photoionization rate and the recombination rate in the H II region becomes equal, the H II region begins to expand owing to the pressure difference between H II region and outer PDR or molecular cloud. At this phase, the SF appears in front of the IF and the IF changes to the weak D-type front (expansion phase). The expansion law in this phase is given by

$$R_{\text{IF}}(t) = R_{\text{st}} \left(1 + \frac{7}{4} \frac{C_{\text{HII}} t}{R_{\text{st}}} \right)^{4/7} \quad (1)$$

(e.g. Spitzer 1978), where C_{HII} is the sound speed in the H II region. The dynamical timescale is now given by $t_{\text{dyn}} = R_{\text{st}}/C_{\text{HII}} \sim 10^5 \text{ yr}$. Fig.1 shows the time evolution of the physical quantities of the gas in the expansion phase. The radius of Sh104 is 4 pc and the IF reaches this radius at $t = 0.7 \text{ Myr}$ in our calculation. For each snapshot, we can see the H II region ($T \sim 10^4 \text{ K}$), the gas shell swept up by the SF ($n_{\text{H}} \sim 10^{4-5} \text{ cm}^{-3}$) and the outer PDR ($T \sim 100 \text{ K}$) and the outermost molecular cloud ($T \sim 10 \text{ K}$). The SF emerges just in front of the IF. The density behind the SF significantly increases from the ambient value owing to the line cooling, and the gas density within the shell is about 10-100 times as high as the ambient density. The more detailed inner structure of the shell is shown below (Fig.3). The geometrical thickness of the shell, h increases throughout the calculation, $h \sim 0.02 - 0.2 \text{ pc}$. The PDR ($T \sim 100 \text{ K}$) becomes narrow as the IF expands, that is, the IF gradually catches

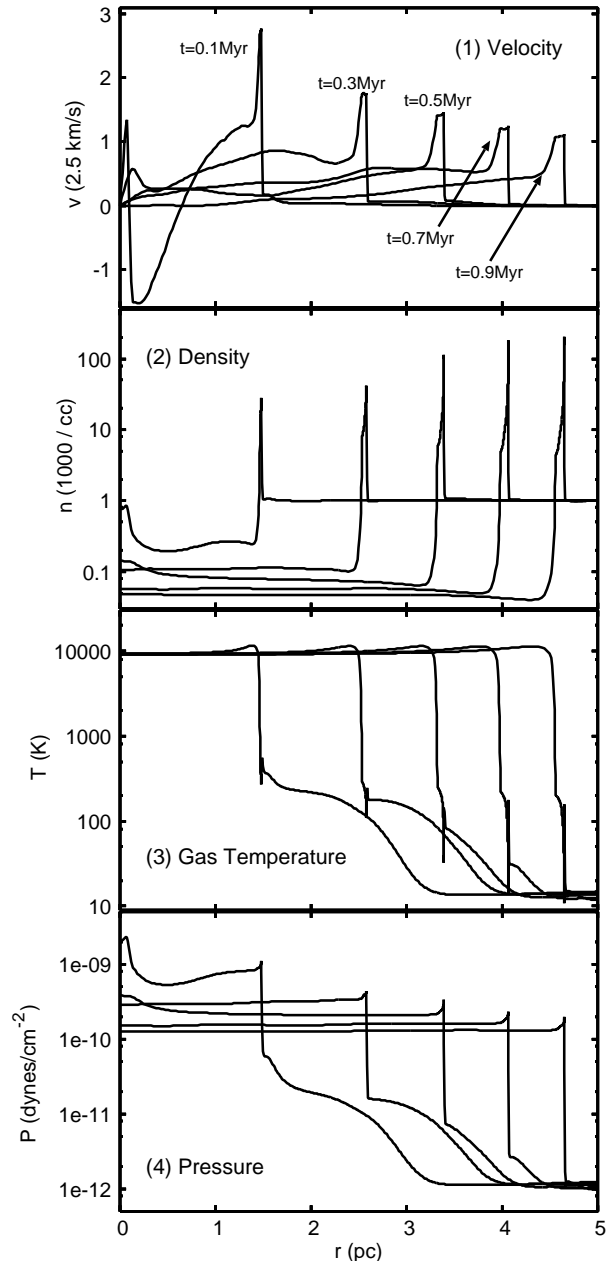


FIG. 1.— The snapshots of the gas-dynamical evolution. In each panel, five snapshots represents the profiles at $t = 0.1, 0.3, 0.5, 0.7,$ and 0.9 Myr respectively.

up with the preceding DFs (e.g. Roger & Dewdney 1992, Diaz-Miller, Franco & Shore 1998). The upper panel of Fig.2 represents the overtaking of the IF more clearly. The position of the SF is very close to that of the IF. As the system switches from the formation phase to the expansion phase, the timescale of the expansion of the IF suddenly becomes longer to t_{dyn} . Even in this phase, the preceding DFs continue to expand. Then the region between IF and DFs appears as a PDR. However, the DFs gradually slow down because the FUV flux at each DF decreases owing to the geometrical dilution and the dust extinction in the PDR. The IF expands because of the pressure difference between the H II region and the outer PDR, and the deceleration is more slower according to eq.(1).

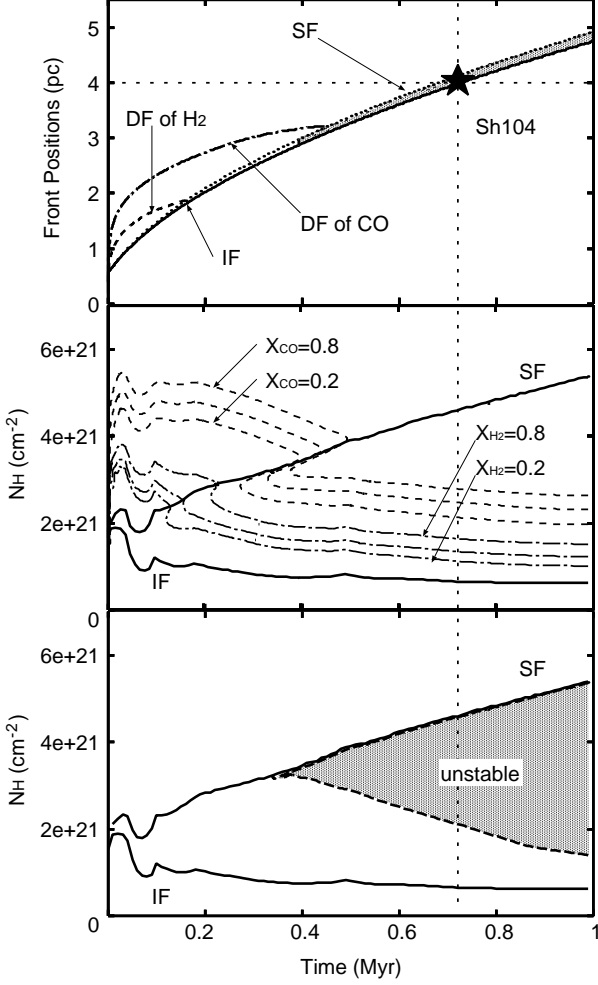


FIG. 2.— *Upper panel* : The time evolution of the various front positions. The solid and dotted lines mean the position of the IF and SF respectively. The broken (dot-solid) line represents the DF of H_2 (CO). To define the DFs of H_2 and CO , we use $X_{H_2} \equiv 2n_{H_2}/n_{H_{nuc}} = 0.5$ and $X_{CO} \equiv n_{CO}/n_{C_{nuc}} = 0.5$. The shaded region corresponds to $t < (G\rho)^{-1/2}$ within the shell, and hence, the gravitational fragmentation is expected (see §4.1). *Middle panel* : The time evolution of the column density of each region. Thin contour lines represent the position where X_{H_2} (broken), X_{CO} (dot-solid) = 0.2, 0.5 and 0.8. *Lower panel* : Same as the middle panel but for showing the gravitationally unstable region. The shaded region corresponds to the region where $t < (G\rho)^{-1/2}$.

The lower two panels of Fig.2 represents the time evolution of the column density of each region. The column density of the H II region gradually decreases because the number density decreases as $n_{HII} \propto R_{IF}^{-3/2}$ in the expansion phase, where R_{IF} is the radius of the H II region. The column density of the gas shell σ increases. The ambient mass swept up by the time t is proportional to $R_{IF}(t)^3$ and the mass within the H II region is $\propto n_{HII}R_{IF}(t)^3 \propto R_{IF}(t)^{3/2}$. Then the most of the swept-up mass does not flow into the H II region but remains in the shell. The calculated mass of the H II region is $430M_{\odot}$ and the shell mass is $9000M_{\odot}$ at $t = 0.7$ Myr (including both PDR and molecular region), which is in good agreement with the observation (see DV03). The PDR initially spreads outside the shell, but H_2 and CO molecules are gradually accumulated from the outer side of the shell. The accumulation of the

molecules already begins when each DF is still outside the

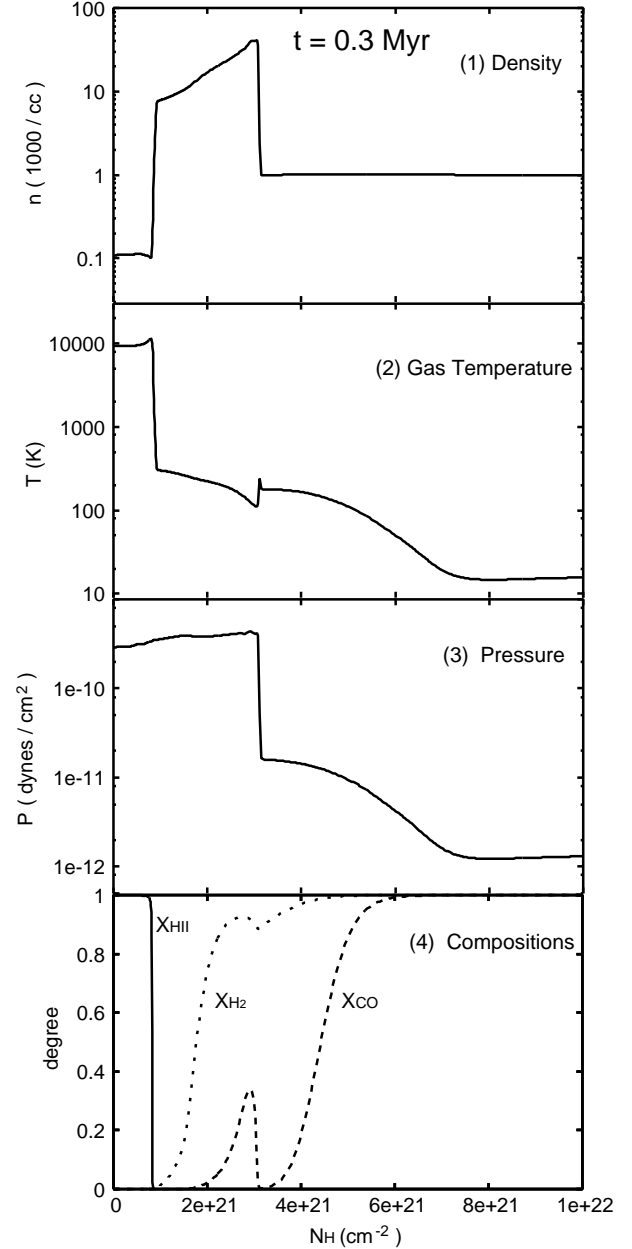


FIG. 3.— The distribution of gas density, pressure, temperature, and the chemical compositions at $t = 0.3$ Myr. In the lowest panel, X_{H_2} and X_{CO} are molecular ratios (see the caption of Fig.2) and X_{HII} is the ionization rate defined as $n_{H^+}/n_{H_{nuc}}$.

SF. Therefore, the accumulation is not simply explained by the fact that the IF and the SF overtakes the DFs and that the SF enters the molecular region. The gas density within the shell is so high that the reformation timescales of the molecules become short enough. The reformation timescale of the hydrogen molecule is about $\sim 10^6$ yr for $n_{H,0} \sim 10^3$ cm^{-3} . The dynamical timescale is about $t_{dyn} \sim 10^5$ yr, then the reformation of H_2 on the grain surface is not important with the ambient number density. However, the reformation timescale in the gas shell, $\sim 10^{4-5}$ yr, is shorter than t_{dyn} , therefore the for-

mation of H_2 molecule is significant in the shell.

Fig.3 shows the detailed structure of the physical quantities and the chemical composition of the shell at $t = 0.3$ Myr. As this figure shows, the molecular fraction in the shell is higher than the value in the PDR outside the shell owing to the rapid reformation. As H II region expands, the DFs are taken in the shell and the denser ($n_{\text{H}} > 10^4 \text{cm}^{-3}$) PDR is formed in the inner side of the shell. Once the molecules are reformed in the shell, the FUV radiation is consumed by the photodissociation of these molecules, which decelerates the expansion of the preceding DFs to accelerates the accumulation of the molecules. About 80 % (55 %) of the hydrogen (carbon) atoms within the shell exist as H_2 (CO) molecule at $t = 0.7$ Myr in our calculation. Fig.3 also shows other interesting features of the shell. The thermal pressure inside the shell is high and about constant at the value of the H II region. The gas temperature has negative gradient from the inner side to the outer side of the shell, because the FUV radiation is attenuated owing to the dust extinction through the shell, and the photoelectric heating decreases. Conversely, the gas density has positive gradient to the outer side of the shell.

4. DISCUSSION

4.1. Dust in H II Region

In this section, we discuss the possible effect of dust grains in the H II regions (e.g. Spitzer 1978). For example, the grains can be driven by the radiation pressure during the expansion of the H II region (e.g., Arthur et al. 2004). Arthur et al. have shown the small grains are destroyed by the sublimation but the large graphite grains can exist close to the star. In contrast, the recent observation by Roger et al. (2004) found no far-infrared component correlated with H II region, Sh170. The photoelectric heating works even in H II regions comparatively with the photoionization heating (Weingartner & Draine 2001) and is sensitive to the uncertain abundance of the small dust grains. If we adopt the dust absorption cross section, $6 \times 10^{-22} \text{cm}^2$ (H nucleon) $^{-1}$ in H II region, which we adopt in the PDR and the outer region, the radius of the H II region becomes slightly smaller, but the difference from the case without dust in H II region is always less than 5%. The temperature in the PDR decreases by 10-20% because of the attenuation of FUV photons by dust grains in the H II region. The gas density within the shell rises by a factor, 1.4-1.5. These changes in the shell, however, only slightly promotes the accumulation of the molecular gas. If we include the standard photoelectric heating rate and dust recombination cooling rate in the H II region (Bakes & Tielens 1994), the temperature near the central star in the H II region rises, but the temperature near the gas shell hardly changes. Therefore, the existence of dust grains do not significantly alter the results in this paper.

4.2. Fragmentation of the Shell

The triggered star formation scenario predicts that the shocked layer fragments and these fragments collapse to stars of the second generation. Although the fragmentation of the shocked layer is studied by many authors, it is still uncertain which instability actually occurs and which

induces the next star formation. Here, we assume that non-gravitational instabilities (e.g. decelerating shock instability (DSI)) themselves are not the essential ones for the sequential star formation. Elmegreen (1989) showed that the gravitational instability couples with DSI for the decelerating layer using the linear analysis, but MacLow & Norman (1993) pointed out that the DSI quickly saturates in the non-linear phase.

However, Garcia-Segura & Franco (1996) showed the DSI is strongly modified with the presence of the IF. The shell rapidly fragments and the finger-like structures are formed in their 2D calculation. Furthermore, the shadowing instability and corrugation instability of the IF were studied by Williams (1999, 2002) and these instabilities also can disturb the IF and the shell. Although these complexities are beyond the scope of this paper, it will be interesting to study the effect of these instabilities on the evolution of the DF and the post-shock layer with 2D or 3D calculations in the future.

Elmegreen & Elmegreen (1978), Miyama, Narita & Hayashi (1987), Lubow & Pringle (1993), and Nagai et al.(1998) have studied the stability of the dense gas layer and show that the earliest gravitational instability occurs with a wavelength which comparable to the layer thickness and the growth rate is $\sim (G\rho)^{-1/2}$. The calculated shell suffers from this instability, and the shaded region in Fig.2 represents the unstable region, where $t \leq (G\rho)^{-1/2}$. Although the mass scale at the maximum growth rate is comparatively small, $\sim \sigma h^2 \sim 1 M_{\odot}$, larger mass scale perturbation gradually grows in turn. As mentioned above, the gas density is higher in the outer part of the shell, then the unstable region extends from the outer edge to the inner part of the shell. By the age of Sh104, 0.7 Myr, the outer part of the shell dominated by CO molecule becomes unstable. Therefore, the dense molecular fragments are formed around H II region and the triggered star formation may occur in the core of them, as DV03 shows.

4.3. The Role of this Triggering Process

Even if the molecular gas is successfully gathered around the H II region and the triggered star formation actually occurs, its impact on the global star formation is still uncertain. However, we can show its significance in a simple argument. In our galaxy, most of stars are formed in clusters (e.g., Evans 1999), then the feedback effects from massive stars are ubiquitous for the global star formation. If every massive star gather the molecular gas of M_{sh} on average and the triggered star formation occurs within the shell, the induced star formation rate SFR_{HII} is estimated as

$$\text{SFR}_{\text{HII}} \sim \text{SFR}_0 \times \left(\frac{M_{\text{av}}}{0.6 M_{\odot}} \right)^{-1} \left(\frac{f(> 20 M_{\odot})}{0.0006} \right) \left(\frac{M_{\text{sh}}}{10^4 M_{\odot}} \right) \left(\frac{\epsilon}{0.1} \right), \quad (2)$$

where SFR_0 is the current total star formation rate in our galaxy, M_{av} is the average stellar mass, $f(> 20 M_{\odot})$ is the number fraction of the massive star which creates relative large H II regions ($> 20 M_{\odot}$), and ϵ is the star formation efficiency for the swept-up gas. The normalization values of $M_{\text{av}} \sim 0.6 M_{\odot}$ and $f(> 20 M_{\odot}) \sim 0.0006$ are calculated with the initial mass function (IMF) given by Miller &

Scalo (1979). Equation (2) shows that if the average mass of the gas shell is $\sim 10^4 M_\odot$, this triggering process even alone can sustain the current galactic star formation rate. In our calculation, the molecular gas of $\sim 10^4 M_\odot$ is accumulated around one massive star owing to the expansion of the H II region by the time of $t \sim 1$ Myr. Therefore, this mode of triggered star formation should be an important process. The efficiency of triggering should depend on the physical conditions, such as type of the central star, ambient density structure and so on. For example, many H II regions show the “blister-like” or “champagne flow” (Tenorio-Tagle 1979) features. In these cases, the IF rapidly erodes the parental cloud and only a part of the swept-up mass remains within the shell, which might result in smaller M_{sh} (e.g., Whitworth 1979, Franco et al. 1994). More realistic estimation including such cases will be explored in Paper II.

5. CONCLUSION

We have calculated the dynamical expansion of H II region and PDR around a massive star, focusing on the dense gas shell around H II region. Our results are simply summarized as follows,

- 1 The dense gas shell is formed just in front of the IF, and this shell is initially atomic but gradually dominated with molecules. This is partly because the IF and SF overtake the preceding DFs and SF enters the molecular region, and partly because the reformation timescale within the shell becomes shorter than the dynamical time because of the high density of the shell.
- 2 The calculation successfully reproduce the observed properties of Sh104. The mass of the shell and H II region, and the location of the IF at $t \sim 0.7$ Myr agree with the observation. The gravitational instability occurs after the gas shell is dominated with the molecular gas. By the time of $t \sim 0.7$ Myr, the gravitationally unstable molecular shell is formed around H II region, as the observation shows.
- 3 In our calculation, the molecular gas shell of the order of $\sim 10^4 M_\odot$ is formed in 1 Myr around one massive star. With simple estimation, we show the triggering process owing to the expansion of H II region is important in context of Galactic star formation.

REFERENCES

- Arthur, S.J., Kurtz, S.E., Franco, J. & Albarran, Y. 2004, ApJ, 608, 282
 Bakes, E.L.O. & Tielens, A.G.G.M. 1994, ApJ, 427, 822
 Deharveng, L. et al. 2003, A&A, 408, 25L
 Diaz-Miller, R.I., Franco, J. & Shore, S.N. 1998, ApJ, 501, 192
 Elmegreen, B.G. & Lada, C.J. 1977, ApJ, 214, 725
 Elmegreen, B.G. & Elmegreen, D.M., 1978, ApJ, 220, 1051
 Elmegreen, B.G. 1989, ApJ, 340, 786
 Elmegreen, B.G., 1998, in Woodward, C.E., Shull, M., Thronson, H.A., eds, ASP Conf.Ser.Vol.148, Origins, Astron.Soc.Pac.San Francisco, p.150
 Evans, N.J.II, 1999, ARA&A, 37, 311
 Franco, J., Shore, S.N. & Tenorio-Tagle, G. 1994, ApJ, 436, 795
 Franco, J., Tenorio-Tagle, G. & Bodenheimer, P. 1990, ApJ, 349, 126
 Garcia-Segura, G. & Franco, J. 1996, ApJ, 469, 171
 Hollenbach, D. & McKee, C.F. 1979, ApJS, 41, 555
 Hollenbach, D. & McKee, C.F. 1989, ApJ, 342, 306
 Hollenbach, D., Takahashi, T. & Tielens, A.G.G.M. 1991, ApJ, 377, 192
 Hosokawa, T. & Inutsuka, S., 2005, in prep. (Paper II)
 Koyama, H. & Inutsuka, S. 2000, ApJ, 532, 980
 Lasker, B.M. 1966, ApJ, 143, 700
 Lubow, S. H. & Pringle, J.E. 1993, MNRAS, 263, 701
 Mac Low, M. & Norman, M.L. 1993, ApJ, 407, 207
 Mathews, W.G. 1965, ApJ, 142, 1120
 Miller, G.E. & Scalo, J.M. 1979, ApJS, 41, 513
 Miyama, S.M., Narita, S. & Hayashi, C. 1987, Prog.Theor.Phys., 78, 105
 Nagai, T., Inutsuka, S. & Miyama, S.M. 1998, ApJ, 506, 306
 Nelson, R.P. & Langer, W.D. 1997, ApJ, 482, 796
 Roger, R.S., McCutcheon, W.H., Purton, C.R. & Dewdney, P.E. 2004, A&A, 425, 553
 Roger, R.S. & Dewdney, P.E. 1992, ApJ, 385, 536
 Spitzer, L. 1978, *Physical Processes in the Interstellar Medium* (New York: Wiley).
 Tenorio-Tagle, G. 1976, A&A, 53, 411
 Tenorio-Tagle, G. 1979, A&A, 71, 59
 van Leer, B. 1979, J.Comput.Phys., 32, 101
 Weingartner, J.C. & Draine, B.T. 2001, ApJ, 548, 296
 Whitworth, A.P. 1979, MNRAS, 186, 59
 Whitworth, A.P., Bhattal, A.S., Chapman, S.J., Disney, M.J., & Turner, J.A. 1994, A&A, 268, 291
 Williams, R.J.R. 1999, MNRAS, 310, 789
 Williams, R.J.R. 2002, MNRAS, 331, 693